Effect of Winding Harmonics on the Asynchronous Torque of a Single-Phase Line-Start Permanent-Magnet Motor

Mircea Popescu TJE Miller Malcolm McGilp
SPEED Laboratory, University of Glasgow, U.K.

F.J.H Kalluf Claudia da Silva Luiz von Dokonal
EMBRACO S.A., Joinville, Brazil

***Abstract*. This paper presents an analytical method for calculating the effect of winding harmonics on the asynchronous torque of a single-phase line-start permanent-magnet motor. The method is an extension of earlier work, which combines symmetrical-component analysis with *dq*-axis theory to model the various components of forward and backward rotating fields. The effect of individual winding harmonics is brought out both theoretically and experimentally, by comparing calculated and measured torque/speed characteristics for a series of six motors with different distributions of turns in both the main and auxiliary windings.**

***Index Terms* – space harmonics, AC motors, capacitor motors, permanent magnet motors, torque simulation, starting**

I. List of Symbols

$\mathbf{V}_m$, $\mathbf{V}_a$ – complex voltages across main and auxiliary windings
$\mathbf{V}_\pm \mathbf{Z}_\pm$ – complex positive/negative sequence voltage and impedance
$\mathbf{V}_{d,q}$, $\mathbf{I}_{d,q}$ – complex *d-q* axis voltage/current components in rotor reference frame
R_s, R_a, R_m – stator winding resistance: equivalent/auxiliary/main
X_{ls} X_{la}, X_{lm} – stator leakage reactance: equivalent/auxiliary/main
β – effective turns ratio (main/auxiliary)
R_{vrd}, R_{vrq} – rotor resistance for ν-th harmonic field in *d-q* axis
X_{vlrd}, X_{vlrq} – rotor leakage reactance for ν-th harmonic field in *d-q* axis
X_{vmd}, X_{vmq} – magnetization reactance for ν-th harmonic field in *d-q* axis
$\mathbf{X}_{vd\pm}$, $\mathbf{X}_{vq\pm}$ – complex positive/negative asynchronous reactance for ν-th harmonic field in *d-q* axis
X_d, X_q – synchronous reactance for fundamental field in *d-q* axis
$\mathbf{Z}_C$ – starting impedance connected in series with auxiliary winding
m, *P* – phases and poles number
ω, *s* – synchronous speed [rad/sec] and slip
ν – harmonics order
kw_{vmain} , kw_{vaux} – main/auxiliary winding factors
E_0 – no-load induced voltage
$A_{m,a}$ – cross-section copper area of the main/auxiliary winding

II. Introduction

There is currently a strong revival of interest in the AC line-start permanent magnet motor for fractional-horsepower applications requiring very high efficiency, such as refrigerator compressors for the high-volume residential market [1-2]. Polyphase variants of this motor have been produced in modest numbers for many years, mainly for specialized industrial applications, but the focus of interest is now on single-phase motors, which have previously not been employed to any significant extent.

The line-start PM synchronous motor has a permanent-magnet rotor with a cage winding similar to that of an induction motor. The single-phase variant has main and auxiliary windings, which operate together with a capacitor to create a rotating flux; see Fig. 1. The cage winding is necessary for starting but it also has the important function of suppressing the negative-sequence flux, as in the induction motor, and this permits the use of a smaller "run" capacitor than would otherwise be necessary, [2].

As in the induction motor, winding harmonics create parasitic torques at all speeds, typically causing "dips" in the torque/speed characteristic, [6-9]. In the PM motor the analysis of these torques is made more complicated by the fact that both the rotor and the stator are asymmetric — the rotor by virtue of the unequal permeances in the *d* and *q* axes, and the stator by virtue of differences in the turn counts and distributions of the main and auxiliary windings, [3]. Additional complications arise from the unbalanced 2-phase supply voltages and from the rotating magnet, which produces not only a braking torque but also a complex set of oscillatory torques due to its interaction with the several harmonic components of the stator ampere-conductor distribution. The oscillatory torques are not only higher, but also persist longer than those in the induction motor, [1, 2, 4, 11, 14].

Earlier analytical methods developed for the polyphase motor [4,5,10,14,19] cannot be used with the single-phase variant [15-18], so this paper extends the analysis of the single-phase motor in [1-2] to include the effect of winding harmonics (also known as "MMF harmonics"). It follows the method described in [1-3] based on a series of reference-frame transformations involving *d-q* axes for the rotor and symmetrical components for the stator, but superimposes an additional set of harmonic components of the MMF distribution. The resulting "harmonic" equivalent circuits bear several similarities to those of Alger [20], but in this case four separate circuits are needed to model both positive and negative sequence components in both the *d* and *q*-axes of the rotor.

Experimental torque/speed curves were obtained for a series of eleven 2-pole, 220/115V, 50/60-Hz capacitor-start, capacitor-run motors with different main and auxiliary winding distributions. The winding distributions were designed to accentuate or minimize particular winding harmonics, in order to determine the separate effects of the principal winding harmonics in the two windings. The same rotor was used in all cases. Comparisons between the theoretical and experimental curves show reasonable agreement, with sufficient correlation to provide important guidance on the overall effect of the winding harmonics and the extent to which imperfections in the winding distribution are tolerable. The speed of calculation is important because of the large number of possible cases requiring analysis and interpretation, justifying the development of an analytical method that is complementary to numerical methods approach.

III. THEORY

Basic structure of the analysis

The unbalanced stator voltage for the case of capacitor- start and/or -run motors affects both the starting and synchronous operation. A suitable combination of the symmetrical components and *d-q* axis theory [1-3], [18] gives accurate results for a detailed analysis of the torque behaviour. The variables are expressed as phasors using complex numbers. Fig. 1 shows the circuit for analysis when a capacitive impedance is series connected with the auxiliary winding. Fig. 2 illustrates the necessary transformations from the actual variables to the proposed model variables. The stator windings are assumed to have the same copper weight and distribution, i.e. $R_s = R_m = \beta^2 R_a$, $X_{ls} = X_{lm} = \beta^2 X_{la}$, $A_a = \beta A_m$. Any differences from this assumption are included in the auxiliary impedance $\mathbf{Z}_C$. If the stator windings are magnetically orthogonal we can transform the actual motor into a symmetrical 2-phase motor:

$$\begin{bmatrix}\mathbf{V}'_a\\ \mathbf{V}'_b\end{bmatrix}=\begin{bmatrix}1 & 0\\ 0 & \frac{1}{\beta}\end{bmatrix}\cdot\begin{bmatrix}\mathbf{V}_a\\ \mathbf{V}_m\end{bmatrix} \tag{1}$$

$$\begin{bmatrix}\mathbf{I}'_a\\ \mathbf{I}'_b\end{bmatrix}=\begin{bmatrix}1 & 0\\ 0 & \beta\end{bmatrix}\cdot\begin{bmatrix}\mathbf{I}_a\\ \mathbf{I}_m\end{bmatrix} \tag{2}$$

The circuit in Fig. 1 is constrained by the equation:

$$\mathbf{V}_s = \mathbf{V}_m = \mathbf{V}_a + \mathbf{Z}_C \cdot \mathbf{I}_a \tag{3}$$

Symmetrical components $\mathbf{V}_+$, $\mathbf{V}_-$, $\mathbf{I}_+$, $\mathbf{I}_-$ are introduced to deal with the supply voltage imbalance. Thus:

$$\begin{bmatrix}\mathbf{V}_+\\ \mathbf{V}_-\end{bmatrix}=\frac{1}{\sqrt{2}}\begin{bmatrix}1 & j\\ 1 & -j\end{bmatrix}\cdot\begin{bmatrix}\mathbf{V}'_a\\ \mathbf{V}'_b\end{bmatrix} \tag{4}$$

with inverse:

$$\begin{bmatrix}\mathbf{V}'_a\\ \mathbf{V}'_b\end{bmatrix}=\frac{1}{\sqrt{2}}\begin{bmatrix}1 & 1\\ -j & j\end{bmatrix}\cdot\begin{bmatrix}\mathbf{V}_+\\ \mathbf{V}_-\end{bmatrix} \tag{5}$$

The same transformation may be applied to the currents. Substituting from eqs. (1), (2), (4) in (3) we get:

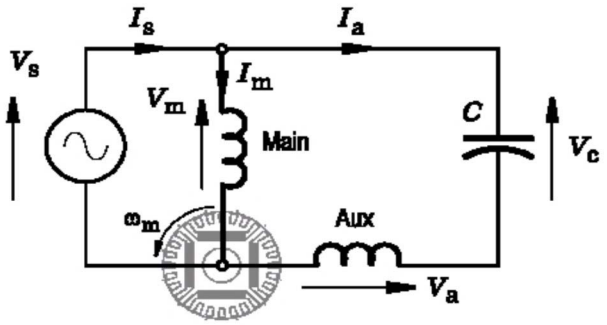

Fig. 1 Circuit for analysis of 1-phase line-start permanent magnet motor with capacitor connection

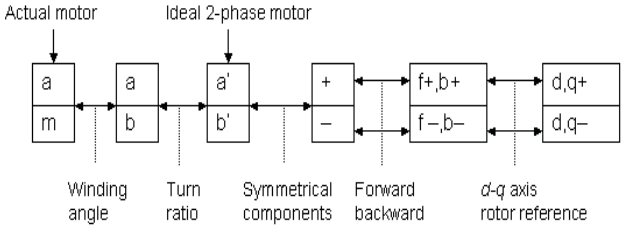

Fig. 2 Transformation from actual voltages and currents to *d-q* axis quantities for 1-phase line-start permanent magnet motor

$$\mathbf{V}_+ = \mathbf{V}_m \cdot \frac{\sqrt{2}}{\beta}\cdot\frac{\beta + j\,\mathbf{a}_2}{\mathbf{a}_1 + \mathbf{a}_2} \quad (6); \quad \mathbf{V}_- = \mathbf{V}_m \cdot \frac{\sqrt{2}}{\beta}\cdot\frac{\beta - j\,\mathbf{a}_1}{\mathbf{a}_1 + \mathbf{a}_2} \quad (7)$$

and

$$\mathbf{V}_+ = \mathbf{Z}_+ \cdot \mathbf{I}_+ \quad (8); \quad \mathbf{V}_- = \mathbf{Z}_- \cdot \mathbf{I}_- \quad (9)$$

where bolded letters stand for complex variables and:

$$\mathbf{a}_1 = 1 + \frac{\mathbf{Z}_C}{\mathbf{Z}_+} \quad (10); \quad \mathbf{a}_2 = 1 + \frac{\mathbf{Z}_C}{\mathbf{Z}_-} \quad (11)$$

Analysis of winding harmonics

For the analysis of winding harmonics, the permeance variation caused by the slot openings is neglected. The space harmonics are of odd order and rotate at subsynchronous speeds in both the forward and reverse directions.

The impedances presented to the positive-sequence (forward) and negative-sequence (backward) harmonic MMF distributions are approximated using the average of the *d* and *q*-axis impedances at the appropriate harmonic frequency. The effect of the equivalent spatial MMF harmonic of order ν may thus be computed using *d*, *q*-axis impedances:

$$\mathbf{Z}_{\nu d\pm} = \frac{1}{\frac{1}{jX_{\nu md}} + \frac{s_{\nu\pm}}{R_{\nu rd} + j\cdot sX_{\nu lrd}}} \tag{12}$$

$$\mathbf{Z}_{\nu q\pm} = \frac{1}{\frac{1}{jX_{\nu mq}} + \frac{s_{\nu\pm}}{R_{\nu rq} + j\cdot sX_{\nu lrq}}} \tag{13}$$

The harmonics slip for positive and negative sequence is defined as a function of the harmonic order ν = 1, -3, 5, -7, … –(4*k* – 1), (4*k* + 1), where *k* = 1, 2, 3, …

$$s_{\nu+} = 1-\nu(1-s)$$
$$s_{\nu-} = 1+\nu(1-s) \tag{14}$$

The magnetization reactance and the rotor leakage reactance for the ν-th harmonic order MMF may be approximated as a function of the reactances corresponding to the fundamental spatial MMF, using winding factors kw_ν:

$$X_{\nu md,q} = \left(\frac{kw_\nu}{kw_1}\right)^2 \frac{X_{1md,q}}{\nu^2}$$
$$X_{\nu lrd,q} = \left(\frac{kw_\nu}{kw_1}\right)^2 \frac{X_{1lrd,q}}{\nu^2} \tag{15}$$

The rotor resistance for higher harmonics is the same as for a motor with ν*P* poles number. Thus, if the rotor bar resistance will be practically unchanged, the rotor ring resistance of the higher order harmonics is diminished with the ratio of ν^2. So, we can use the approximation:

$$R_{\nu rd,q} = R_{rd,q\_bar} + \frac{R_{rd,q\_ring}}{\nu^2} \approx R_{lrd,q} \tag{16}$$

The total impedance of the positive and negative sequence is:

$$\mathbf{Z}_+ = R_s + jX_{ls} + \frac{1}{2}\cdot\sum_{\nu=1}^{N}\left(\mathbf{Z}_{\nu d+} + \mathbf{Z}_{\nu q+}\right) \tag{17}$$

$$\mathbf{Z}_- = R_s + jX_{ls} + \frac{1}{2}\cdot\sum_{\nu=1}^{N}\left(\mathbf{Z}_{\nu d-} + \mathbf{Z}_{\nu q-}\right) \tag{18}$$

where *N* is the number of considered harmonics order.

The unbalanced supply voltage system can be further decomposed into an orthogonal system (*d-q*) using symmetrical components as in [3].

The positive sequence $\mathbf{V}_+$ will induce currents in the cage rotor of the line-start permanent magnet motor. If *f* is the fundamental supply frequency, the frequency of the rotor currents will be *sf*. In a similar way, the negative sequence $\mathbf{V}_-$ will induce currents in the cage rotor, with frequency (2-*s*)*f*. In double revolving field theory, currents with frequency *sf* determine the forward field, and the currents of frequency (2-*s*)*f* determine the backward field. Thus, the initial unbalanced line-start permanent magnet motor is equivalent to two stator-balanced motors. Each of these fictitious motors is characterised by an asymmetrical rotor configuration, due to the cage and the permanent magnets.

Solution of the voltage equations

Using the *d-q* axis fixed on the rotor frame, we can write the following linear differential stator voltage equations for the positive sequence motor:

$$\mathbf{V}_{d+} = \mathbf{V}_+ = R_s\mathbf{I}_{d+} + j\omega\sum_{\nu=1}^{N}\left(s_{\nu+}\boldsymbol{\psi}_{\nu d+}\right) - \omega(1-s)\sum_{\nu=1}^{N}\left(\boldsymbol{\psi}_{\nu q+}\right) \tag{19}$$

$$\mathbf{V}_{q+} = -j\mathbf{V}_+ = R_s\mathbf{I}_{q+} + j\omega\sum_{\nu=1}^{N}\left(s_{\nu+}\boldsymbol{\psi}_{\nu q+}\right) + \omega(1-s)\sum_{\nu=1}^{N}\left(\boldsymbol{\psi}_{\nu d+}\right) \tag{20}$$

and for the negative sequence motor:

$$\mathbf{V}_{d-} = \mathbf{V}_- = R_s\mathbf{I}_{d-} + j\omega\sum_{\nu=1}^{N}\left(s_{\nu-}\boldsymbol{\psi}_{\nu d-}\right) - \omega(1-s)\sum_{\nu=1}^{N}\left(\boldsymbol{\psi}_{\nu q-}\right) \tag{21}$$

$$\mathbf{V}_{q-} = j\mathbf{V}_- = R_s\mathbf{I}_{q-} + j\omega\sum_{\nu=1}^{N}\left(s_{\nu-}\boldsymbol{\psi}_{\nu q-}\right) + \omega(1-s)\sum_{\nu=1}^{N}\left(\boldsymbol{\psi}_{\nu d-}\right) \tag{22}$$

For the flux linkage components we will use the notations:

$$\omega\boldsymbol{\psi}_{\nu d\pm} = \mathbf{X}_{\nu d\pm}(js)\mathbf{I}_{d\pm} = -j\mathbf{Z}_{\nu d\pm}\mathbf{I}_{d\pm} \tag{23}$$

$$\omega\boldsymbol{\psi}_{\nu q\pm} = \mathbf{X}_{\nu q\pm}(js)\mathbf{I}_{q\pm} = -j\mathbf{Z}_{\nu q\pm}\mathbf{I}_{q\pm} \tag{24}$$

Introducing (23) and (24) in (19), (20) and respectively in (21), (22) and solving the equation systems, we may obtain the following equivalent relationships for *d*+, *d*– and *q*+, *q*– axis currents. These relationships are also expressed in the form of equivalent circuits for the various components in Figs. 3 and 4.

Positive sequence:

$$\mathbf{I}_{d+} = \frac{\mathbf{V}_+}{D_+}\left[R_s + j\sum_{\nu=1}^{N}\left(s_{\nu+}\mathbf{X}_{\nu q+}\right) - j(1-s)\sum_{\nu=1}^{N}\left(\mathbf{X}_{\nu q+}\right)\right] \tag{25}$$

$$\mathbf{I}_{q+} = -\frac{j\mathbf{V}_+}{D_+}\left[R_s + j\sum_{\nu=1}^{N}\left(s_{\nu+}\mathbf{X}_{\nu d+}\right) - j(1-s)\sum_{\nu=1}^{N}\left(\mathbf{X}_{\nu d+}\right)\right] \tag{26}$$

Negative sequence*:*

$$\mathbf{I}_{d-} = \frac{\mathbf{V}_-}{D_-}\left[R_s + j\sum_{\nu=1}^{N}\left(s_{\nu-}\mathbf{X}_{\nu q-}\right) - j(1-s)\sum_{\nu=1}^{N}\left(\mathbf{X}_{\nu q-}\right)\right] \tag{27}$$

$$\mathbf{I}_{q-} = \frac{j\mathbf{V}_-}{D_-}\left[R_s + j\sum_{\nu=1}^{N}\left(s_{\nu-}\mathbf{X}_{\nu d-}\right) - j(1-s)\sum_{\nu=1}^{N}\left(\mathbf{X}_{\nu d-}\right)\right] \tag{28}$$

where:

$$D_+ = R_s^2 + (1-s)^2\sum_{\nu=1}^{N}\left(\mathbf{X}_{\nu d+}\mathbf{X}_{\nu q+}\right) + \sum_{\nu=1}^{N}\left[\left(s_{\nu+}\right)^2\mathbf{X}_{\nu d+}\mathbf{X}_{\nu q+}\right] + jR_s\left(\sum_{\nu=1}^{N}s_{\nu+}\mathbf{X}_{\nu d+} + \sum_{\nu=1}^{N}s_{\nu+}\mathbf{X}_{\nu q+}\right) \tag{29}$$

$$D_- = R_s^2 + (1-s)^2\sum_{\nu=1}^{N}\left(\mathbf{X}_{\nu d-}\mathbf{X}_{\nu q-}\right) + \sum_{\nu=1}^{N}\left[\left(s_{\nu-}\right)^2\mathbf{X}_{\nu d-}\mathbf{X}_{\nu q-}\right] + jR_s\left(\sum_{\nu=1}^{N}s_{\nu-}\mathbf{X}_{\nu d-} + \sum_{\nu=1}^{N}s_{\nu-}\mathbf{X}_{\nu q-}\right) \tag{30}$$

Harmonics asynchronous cage torques

The individual contribution of each space MMF harmonic to the electromagnetic torque production can be identified.

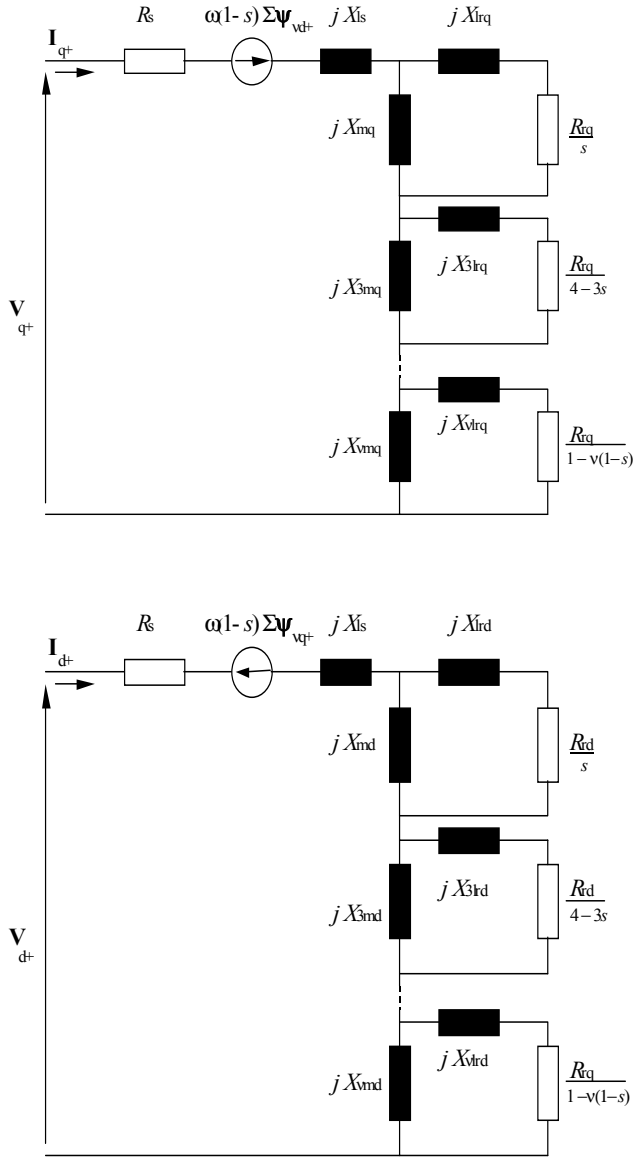

Fig. 3. Single-phase line-start permanent magnet motor positive sequence equivalent circuit for cage torque computation –with odd MMF harmonics

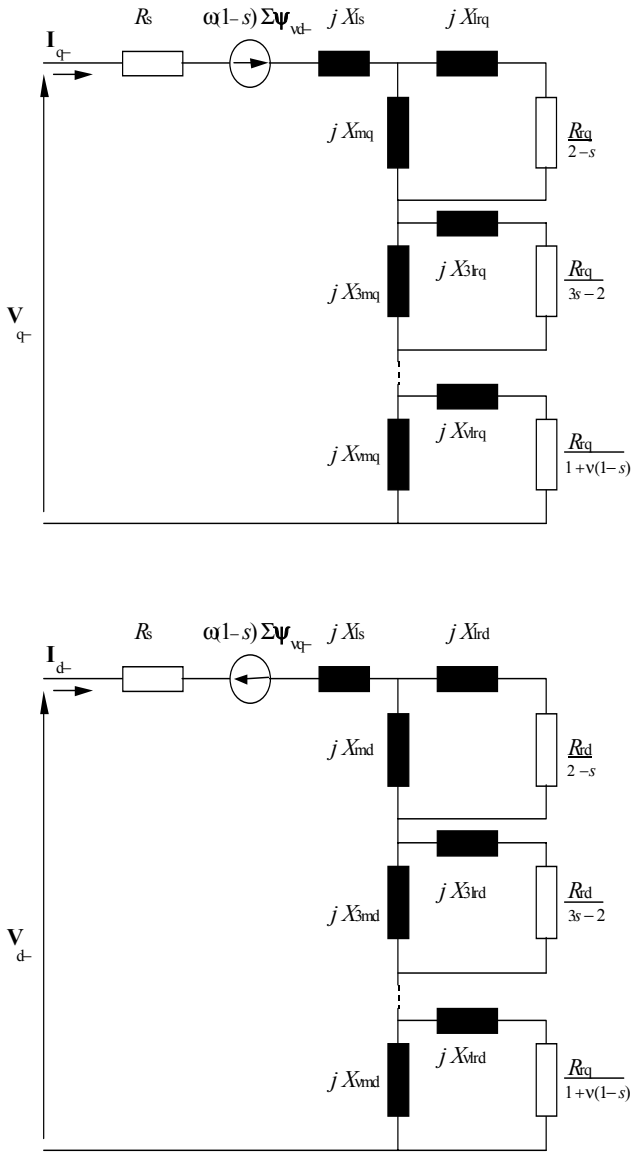

Fig. 4. Single-phase line-start permanent magnet motor negative sequence equivalent circuit for cage torque computation –with odd MMF harmonics

The following relations compute the air-gap average asynchronous cage torque components (positive and negative sequence) valid for a 1-phase AC motor with unbalanced stator voltage:

$$T_{(\text{cage})+} = \frac{P}{2} \cdot \sum_{\nu=1}^{N} \nu \,\text{Re}\left[\left(\boldsymbol{\psi}_{\nu \text{q}+} \right)^{*} \mathbf{I}_{\text{d}+} - \left(\boldsymbol{\psi}_{\nu \text{d}+} \right)^{*} \mathbf{I}_{\text{q}+} \right] \tag{31}$$

$$T_{(\text{cage})-} = \frac{P}{2} \cdot \sum_{\nu=1}^{N} \nu \,\text{Re}\left[\left(\boldsymbol{\psi}_{\nu \text{q}-} \right)^{*} \mathbf{I}_{\text{d}-} - \left(\boldsymbol{\psi}_{\nu \text{d}-} \right)^{*} \mathbf{I}_{\text{q}-} \right] \tag{32}$$

For higher order harmonics, the torque must be multiplied by the order of the harmonic. The ν-th harmonic field produces a torque similar to a motor with ν times the number of poles of the fundamental field. Usually, the auxiliary winding is displaced 90 electrical degrees from the main winding of the fundamental. This displacement is ν times 90 electrical degrees for the ν-th harmonic. The total average cage torque will be defined as:

$$T_{(\text{avg})} = T_{(\text{cage})+} + T_{(\text{cage})-} \tag{33}$$

For the case of a balanced 2-phase motor, only the positive sequence cage torque $T_{(cage)+}$ is present. The harmonics torque of order $\nu = (4k-1)$ will rotate in opposite sense with the fundamental flux wave, while harmonics torque of order $\nu = (4k+1)$ rotate in the same sense with the fundamental. One drawback of the previously described equivalent circuits is that they employ fixed value parameters. The reactances, especially the *d-q* axes harmonics synchronous values ($\mathbf{X}_{\nu d\pm}$, $\mathbf{X}_{\nu q\pm}$) are subjected to strong saturation level. Saturation of the magnetic circuit is particularly complex in line-start permanent magnet motor: different sections of the machine saturate independently, causing large and sometimes time-varying changes in equivalent circuit parameters such as inductances and back EMF. Therefore, the developed model used average saturated values for the *d-q* axes inductances corresponding to the fundamental flux wave and the open- circuit value for the back EMF. The harmonics inductances are determined from the fundamental values using (15). Usually, for single-phase line-start PM motors the auxiliary winding exhibits a more important space harmonics content. In this case the equivalent circuits in Figs. 3 and 4 contain elements referred to the auxiliary winding by multiplying the resistances and reactances to $1/\beta^2$ and using the corresponding winding factors ($kw_{\nu aux}$). The induced voltage E_0 is scaled with $\sqrt{2}/\beta$ [2]. When harmonics content is relevant in both stator windings, an initial torque is computed assuming space harmonics just in the main winding ($kw_{\nu main}$). Then the equivalent circuits are solved using elements referred to the auxiliary winding and assuming space harmonics just in the auxiliary winding ($kw_{\nu aux}$). Thus, a second torque value is obtained. The resultant cage torque will be estimated as an average between these two torque values.

Asynchronous magnet braking torque

During asynchronous operation, the accelerating torque of the line-start permanent magnet motor is the average cage torque minus the magnet braking torque and the load torque. The magnet braking torque is produced by the fact that the magnet flux generates currents in the stator windings, and is associated with the loss in the stator circuit resistance. The magnet braking torque should not be confused with the synchronous "alignment" torque that arises at synchronous speed, even though the magnet braking torque is still present at synchronous speed and therefore diminishes output and efficiency. A complete *d-q* axis analysis of the magnet braking torque for a 3-phase symmetrical line-start permanent magnet motor is given in [4] and in [14]. The average air-gap magnet braking torque for a single-phase variant is defined as [1]:

$$T_m = \frac{P}{2}\cdot\left[\frac{1}{\beta}\cdot\psi_{dm} I_{qm} - \beta\cdot\psi_{qm} I_{dm}\right] \tag{34}$$

The average air-gap resultant electromagnetic torque will be given by:

$$T_e = T_{(avg)} + T_m \tag{35}$$

IV. Comparison with Experimental Data

The proposed analytical method is validated on two groups of motors with identical cross section (24 slots/28 bars) and stack length, but with different stator windings. First group comprises six motors with 2-pole, 220V, 50Hz. For this set of motors the effective turns ratio β (main/auxiliary) was kept constant, while the total number of turns per phase and winding distribution are changed. Second group comprises five motors with 2-pole, 115V, 60Hz. For this set of motors the effective turns ratio β (main/auxiliary) has a different value for each motor. The main winding is quasi sinewave distributed, but with different total number of turns per phase. The auxiliary winding exhibits different space MMF harmonics content, but with the total number of turns per phase kept almost constant. In Table I the winding factors up to the 7th space harmonic for the first group of tested motors are presented, where $kw_{\nu main}$ and $kw_{\nu aux}$ stand for main and auxiliary windings harmonics factors. Similarly, in Table II the winding factors up to the 7th space harmonic for the second group of tested motors are presented. Tests were performed for 90% rated voltage, i.e., 198Vrms line voltage for the first motor group and 103Vrms line voltage for the second motor group. The winding temperature was 80°C in all cases. Starting capacitors are always connected during tests and their values were: 58μF for the first group of tested motors, and 150,200,250 μF for the second group of tested motors.

Figs 5 and 6 show the measured torques vs speed, and Figs. 7, 8, 9 illustrate the currents variation during starting.

Considering the harmonics windings factors the analysed motors exhibit different content of space MMF harmonics, and thus the average torque is modified from one case to another. Note the significant decrease of the average asynchronous torque when the auxiliary winding exhibits important space MMF harmonics content (Motor 4, 5, 6 in first group – Fig. 5, and Motor 7, Motor 8 in second group – Fig. 6). The presence of space harmonics in the field created by the auxiliary winding leads to an increased backward revolving field and consequently to a decreased average asynchronous torque. As expected, the best performance occurred for the case when stator is equipped with quasi sinewave distributed windings, i.e., Motor 4 and Motor 11. Tests performed on the second motor group demonstrate the posibility of increasing the starting torque by decreasing the effective turns ratio β (main/auxiliary) for the same start capacitor value. The stator currents amplitude during starting tests showed a similar pattern with the starting torque, i.e., an increased amplitude when the effective turns ratio β (main/auxiliary) is decreased. Also, the presence of an important space MMF harmonics content (e.g. Motor 7, Motor 8) apparently shifts the maximum value of the magnet braking torque toward a higher speed. The differences between test data and computation that still occur can be explained by the fact that the reactances value varies from locked-rotor to synchronous operation conditions due to the saturation level.

TABLE I
WINDING FACTORS FOR FIRST GROUP OF TESTED MOTORS
2-POLE, 220V, 50HZ. CSTART=58μF

Winding data	Motor 1	Motor 2	Motor 3	Motor 4	Motor 5	Motor 6
kw_{1main}	0.804	0.8477	0.900	0.8289	0.8289	0.8289
kw_{3main}	0.0117	0.1776	0.374	0.0646	0.0646	0.0646
kw_{5main}	0.0086	0.0021	0.003	0.0709	0.0709	0.0709
kw_{7main}	0.0224	0.0536	0.1252	0.0405	0.0405	0.0405
kw_{1aux}	0.8545	0.8545	0.8545	0.8478	0.8914	0.9273
kw_{3aux}	0.1074	0.1074	0.1074	0.082	0.274	0.4626
kw_{5aux}	0.1635	0.1635	0.1635	0.1642	0.1388	0.0179
kw_{7aux}	0.1026	0.1026	0.1026	0.0861	0.0707	0.174
β	1.37	1.37	1.37	1.37	1.37	1.37

TABLE II
WINDING FACTORS FOR SECOND GROUP OF TESTED MOTORS
2-POLE, 115V, 60HZ

Winding data	Motor 7	Motor 8	Motor 9	Motor 10	Motor 11
kw_{1main}	0.8189	0.8218	0.8257	0.8238	0.8166
kw_{3main}	0.0426	0.043	0.0718	0.0793	0.0234
kw_{5main}	0.0416	0.0554	0.0336	0.0117	0.0348
kw_{7main}	0.0419	0.0575	0.0278	0.0076	0.0313
kw_{1aux}	0.8727	0.8727	0.8671	0.8443	0.8484
kw_{3aux}	0.2027	0.2027	0.1684	0.0652	0.0903
kw_{5aux}	0.1212	0.1212	0.1556	0.1668	0.1425
kw_{7aux}	0.0391	0.0391	0.0235	0.1075	0.0878
β	1.7	1.61	1.54	1.36	1.29
Cstart [μF]	150	150	200	200	250

The computed results are obtained using fixed-value reactances corresponding to the saturation level that occurs at synchronous speed, rated load conditions. A magnetostatic finite element analysis [21] showed that during starting the *dq* axis reactances (X_d, X_q) may experience a strong saturation, in a ratio of up to 3:1 as compared to the values estimated for linear cases.

Due to space limitations, we present the comparison between test data and computed results for the asynchronous torque of the following illustrative motors:

(a) Motor 1 – low content of space MMF harmonics in both stator windings (Fig. 10, Table I); (b) Motor 3 – high 3rd harmonic content in main winding and quasi sinewave distributed auxiliary winding (Fig. 11, Table I); (c) Motor 6 – high 3rd harmonic content in auxiliary winding and quasi sinewave distributed main winding (Fig. 12, Table I); (d) Motor 7 – high space MMF harmonic content in auxiliary winding and quasi sinewave distributed main winding (Fig. 13, Table II); (e) Motor 8 – similar winding distribution to Motor 7, but with decreased turns ratio (Fig. 14, Table II); (f) Motor 11 – low content of space MMF harmonics in both stator windings (Fig. 15, Table II).

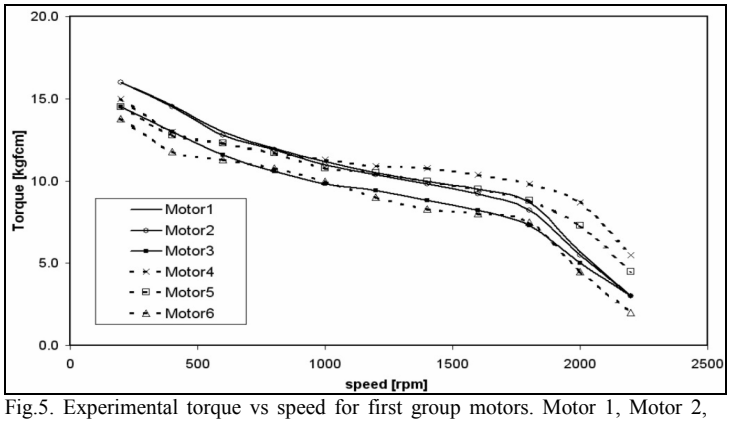

Fig.5. Experimental torque vs speed for first group motors. Motor 1, Motor 2, Motor 3 have space MMF harmonics in main winding, Motor 4, Motor 5, Motor 6 have space MMF harmonics in auxiliary winding. (see Table I)

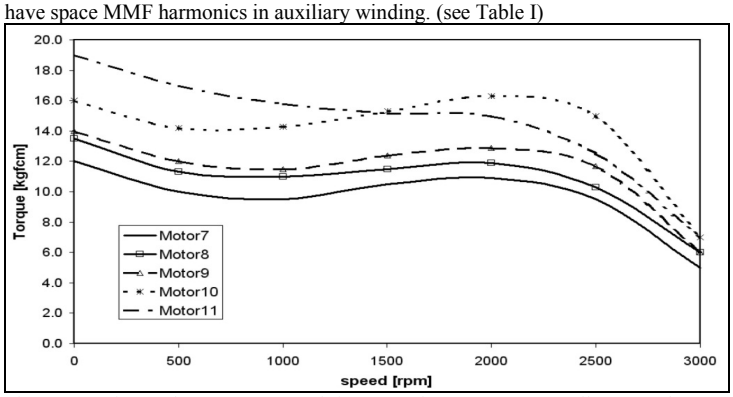

Fig.6. Experimental torque vs speed for second group motors. All motors have space MMF harmonics in auxiliary winding. (see Table II)

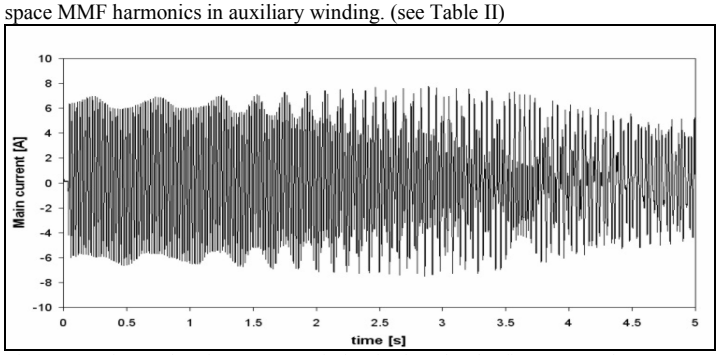

Fig. 7 Experimental main current variation in time for the first group of motors

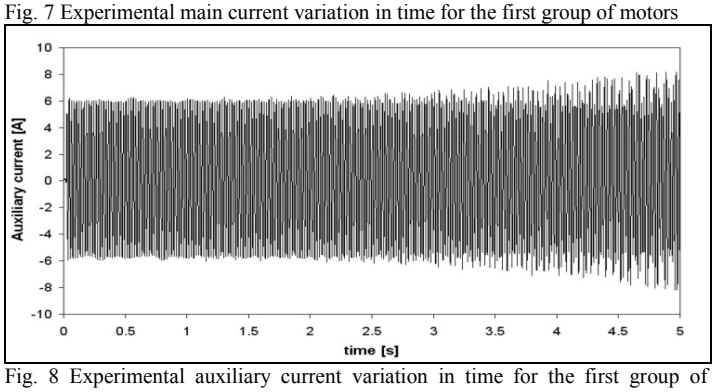

Fig. 8 Experimental auxiliary current variation in time for the first group of motors

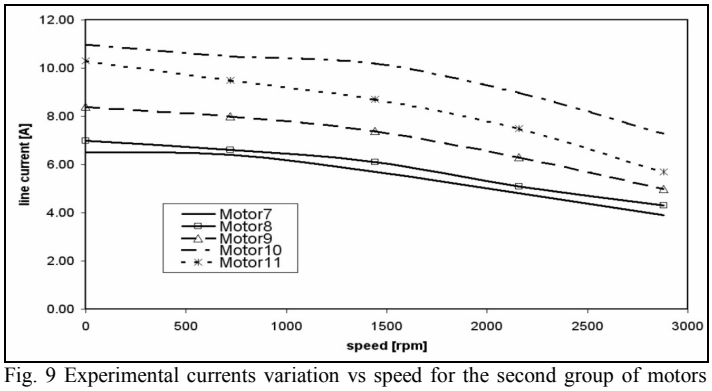

Fig. 9 Experimental currents variation vs speed for the second group of motors (see Table II)

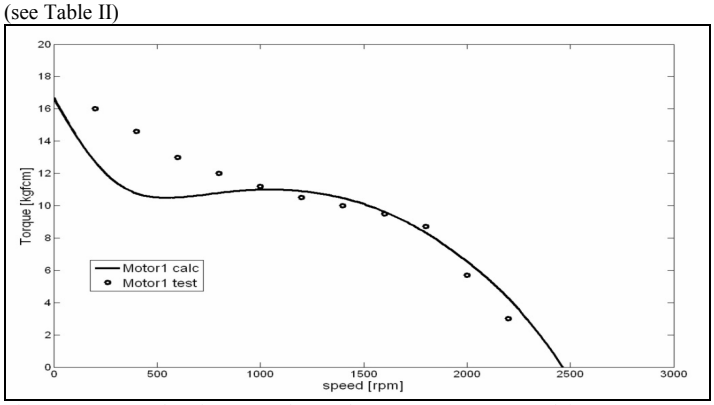

Fig. 10. Computed and measured asynchronous torque vs speed for Motor 1 (see Table I).

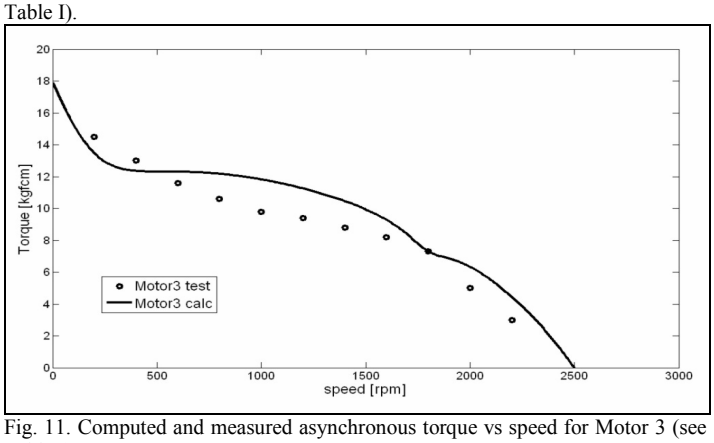

Fig. 11. Computed and measured asynchronous torque vs speed for Motor 3 (see Table I).

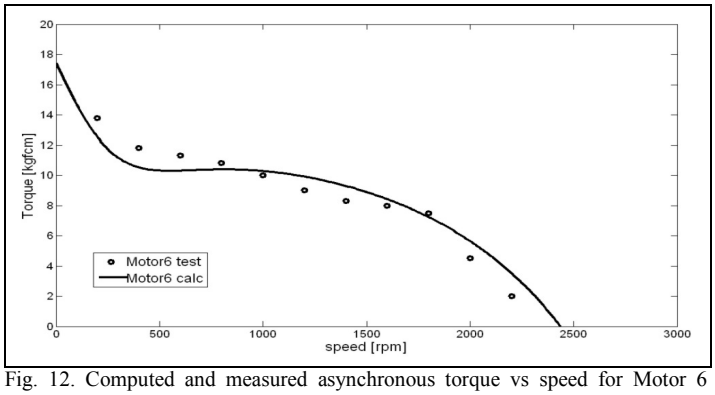

Fig. 12. Computed and measured asynchronous torque vs speed for Motor 6 (Table I).

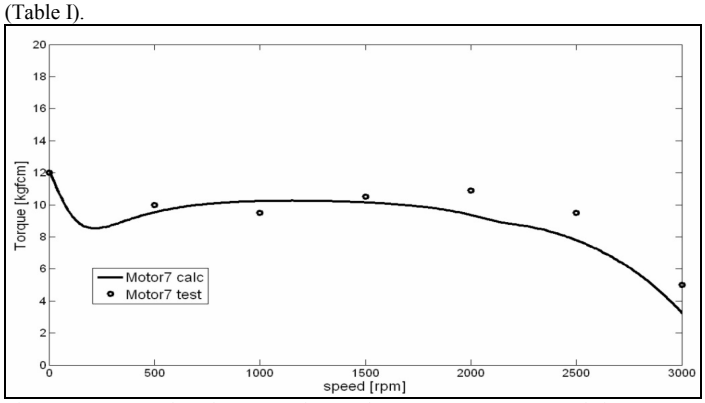

Fig. 13. Computed and measured asynchronous torque vs speed for Motor 7 (Table II).

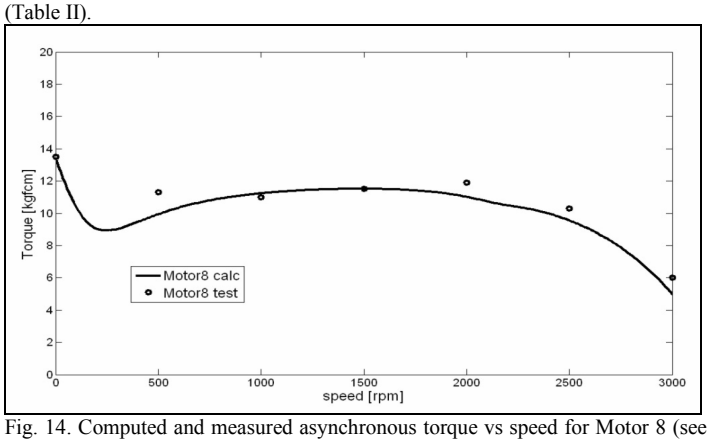

Fig. 14. Computed and measured asynchronous torque vs speed for Motor 8 (see Table II).

The first group of analysed motors, showed that the space MMF harmonics presence will have a small impact on the starting torque value, but will determine a decreased average asynchronous torque for almost the entire range of speed. The space harmonics created by the auxiliary winding distribution tend to determine a flat aspect of the torque variation vs. speed during starting. Fig. 16 illustrates the variation of harmonic torques vs slip for one of the tested motors.

The second group of analysed motors, validated the assumption that the turns ratio influences the starting torque value, but as well the magnet braking torque.

By decreasing the turns ratio (β) and using similar or smaller starting reactance ($\mathbf{Z}_C$), the starting torque may be increased (Fig. 17), while the magnet braking torque is minimised. The starting line current will follow the same pattern as the starting torque. Depending on the application requirements, the value for the effective turns ratio (main/auxiliary) may be optimised. If the auxiliary winding is necessary just for starting, $\beta \geq 1$. If the auxiliary winding is necessary for starting and synchronous operation, i.e. the motor will operate close to a 2-phase balanced conditions system, then $\beta < 1$.

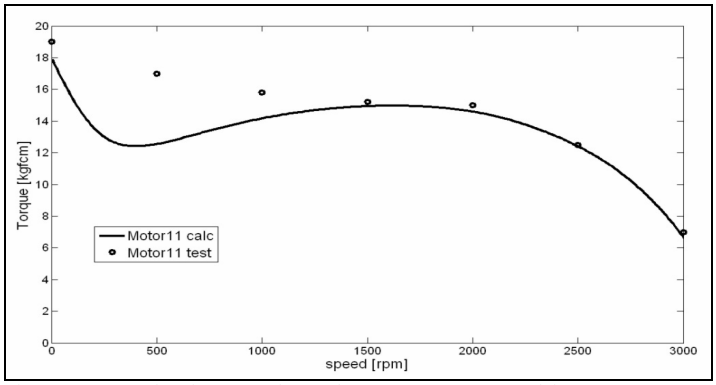

Fig. 15 Computed and measured asynchronous torque vs speed for Motor 11.

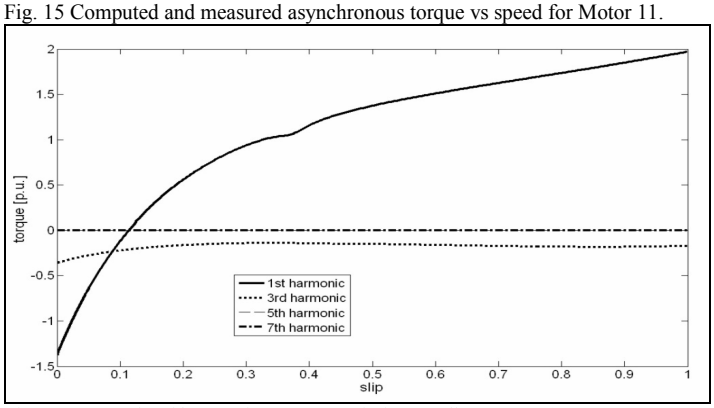

Fig. 16. Example of harmonic torques variation vs slip (Motor 3)

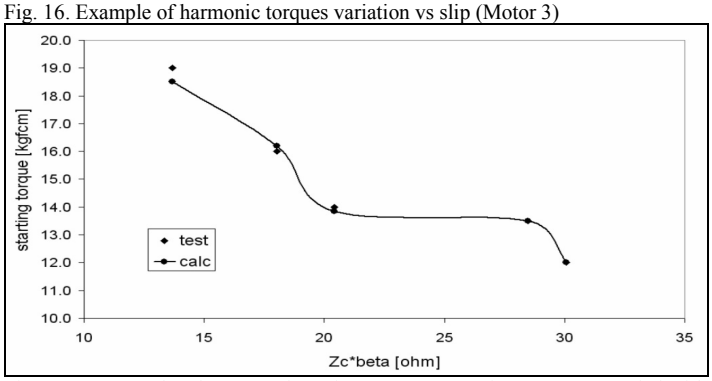

Fig. 17. Computed and measured starting torque vs starting reactance scaled with turns ratio $\mathbf{Z}_c$*β (see Table II).

V. CONCLUSIONS

The experimental data show that winding harmonics in the both the main auxiliary winding can have a significant effect on the asynchronous torque. The extended theoretical model based on symmetrical components with time-averaged *dq* axis impedances correlates well with the measured torque/speed characteristics of the test motor, providing important theoretical guidance to the level of winding harmonics. The effects are more complex than in single-phase induction motors and modify the average asynchronous torque values for the entire range of speed. An optimised value for the effective turns ratio is essential when the motor performance need to be maximised.

REFERENCES

[1]. Popescu, M., Miller, T.J.E., McGilp, M.I., Strappazzon, G., Trivillin, N., Santarossa, R.: "Line Start Permanent Magnet Motor: Single-Phase Starting Performance Analysis" –*IEEE Transactions on Ind. Appl.*, Vol. 39, No. 4, July-August 2003, pp. 1021 – 1030

[2]. Miller, T.J.E., Popescu, M., Cossar, C., McGilp, M.I., Strappazzon, G., Trivillin, N., Santarossa, R.: "Line Start Permanent Magnet Motor: Single-Phase Steady-state Performance Analysis" –*IEEE Transactions on Ind. Appl.*, Vol. 40, No. 2, March-April 2004, pp. 516 – 525

[3]. Miller, T.J.E. "Single-phase permanent magnet motor analysis", *IEEE Trans. Ind. Appl.*, Vol. IA-21, pp. 651-658, May-June 1985

[4]. Honsinger, V.B. "Permanent magnet machine: Asynchronous operation", *IEEE Trans. Power Appl. Syst.*, vol. PAS-99, pp.1503-1509, July 1980

[5]. Miller, T.J.E. "Synchronisation of line-start permanent magnet motors" *IEEE Transactions on Power Apparatus and Systems*, Vol. PAS-103, no. 7, July 1984, pp. 1822-1828

[6]. Buchanan, L.W. "An equivalent circuit for a single-phase motor having space harmonics in its magnetic field" *IEEE Transactions*, *PAS-84*, November 1965, pp. 999 – 1007

[7]. Davis J. H. and Novotny D. W. "Equivalent circuits for single-phase squirrel-cage induction machines with both odd and even order MMF harmonics" *IEEE PAS-88*, July 1969, pp. 1080 – 1086

[8]. Heartz, R.P. and Saunders R.M, "Harmonics due to slots in electric machines" *AIEE Trans. (Power Apparatus System)* August 1954, Vol. 73, pp. 946-949

[9]. Fudeh H. R. and Ong C. M., "Modeling and analysis of induction machines containing space harmonics" Part I, II, III, *IEEE PAS-102*, August 1983, pp. 2608 - 2628

[10]. Miyashita, K., Yamashita, S., Tanabe, S., Shimozu, T., Sento, H.: "Development of a high-speed 2-pole permanent magnet synchronous motor" *IEEE Trans. on Power Apparatus and Systems*, Vol. PAS-99, No. 6, Nov/Dec. 1980, pp. 2175 – 2183

[11]. Williamson, S.; Knight, A.M. "Performance of skewed single-phase line-start permanent magnet motors" *IEEE Transactions on Ind. Appl.* , Vol. 35, pp. 577 –582, May-June 1999

[12]. Stephens, C.M.; Kliman, G.B.; Boyd, J. "A line-start permanent magnet motor with gentle starting behavior" *Industry Applications Conference, 1998. Thirty-Third IAS Annual Meeting. The 1998 IEEE*, Vol. 1, pp. 371 –379, 1998

[13]. Chalmers, B.J.; Baines, G.D.; Williamson, A.C. "Performance of a line-start single-phase permanent-magnet synchronous motor" *Electrical Machines and Drives, 1995. Seventh International Conference on*, pp. 413-417, 1995

[14]. Rahman, M.A.; Osheiba, A.M. "Performance of large line-start permanent magnet synchronous motors", *IEEE Transactions on En. Conv.*, Vol. 5, pp. 211-217, March 1990

[15]. Zhou J, Tseng K-J. "Performance analysis of single-phase line-start permanent magnet synchronous motor", *IEEE Transactions on En. Conv.*, Vol. 17, No. 4, pp. 453-462, December 2002

[16]. Kang G-H, Lee B-K., Nam H., Hur J., Hong J-P. "Analysis of single-phase line-start permanent-magnet motor considering iron loss and parameter variation with load angle", *IEEE Transactions on Industry Applications*, Vol. 40, No: 3, pp: 797- 805, May-June 2004

[17]. Carlson, R.; Sadowski, N.; Arruda, S.R.; Da Silva, C.A.; Von Dokonal, L. "Single-phase line-started permanent magnet motor analysis using finite element method" *Industry Applications Society Annual Meeting,*, 1994, Vol. 1, pp 227 - 233

[18] Boldea, I., Dumitrescu, T., Nasar, S. "Unified analysis of 1-phase AC motors having capacitors in auxiliary windings" *Energy Conversion IEEE Transactions on*, Vol. 14, No.3, September 1999, pp. 577-58

[19] Miller TJE "Transient performance of permanent-magnet AC machines". *Industry Applications Society Annual Meeting*, 1981, pp.500-503

[20] Alger PL *Induction machines, their behavior and uses*, Gordon & Breach Science Publishers, New York, London, Paris, Second Edition, 1970

[21] Miller TJE, Popescu M., McGilp M.I., Cossar, C., Walker J.A. "Calculating the interior permanent magnet motor"– *Conf. Rec. IEEE IEMDC'03*, June 2003, Madison, USA, pp. 1181-1187